Oxidation of CO by SO_2: A Theoretical Study

George B. Bacskay and John C. Mackie*

School of Chemistry, University of Sydney, NSW 2006, Australia

Received: October 28, 2004; In Final Form: January 3, 2005

The elementary reaction $SO_2 + CO \rightarrow CO_2 + SO(^3\Sigma)$ (1) and the subsequent reaction $SO(^3\Sigma) + CO \rightarrow CO_2 + S(^3P)$ (2) have been studied by the application of the Gaussian-3//B3LYP quantum chemical approach to characterize the potential energy surfaces and transition state kinetic analysis to derive rate coefficients. Reaction 1 is found to take place via two transition states (TS), a *cis*-OSOCO TS and a *trans*-OSOCO TS. Reaction via the *cis*-TS is concerted and takes place on a singlet surface. Intersystem crossing to the final products occurs after passage through the barrier on the singlet surface. The *trans*-TS leads to a very weakly bound singlet OSOCO intermediate that then passes through a second TS (on the triplet surface) to form the products. Reaction 2 takes place on triplet surfaces. There is a concerted reaction through a *cis*-SOCO TS and a weakly bound *trans*-SOCO has also been identified. Reaction 2 is analogous to the reaction $CO + O_2(^3\Sigma) \rightarrow CO_2 + O(^3P)$ (3), and this reaction has been reinvestigated at a similar level of theory and the rate coefficient derived by quantum chemistry is compared with experiment. The sensitive effects of trace impurities such as H_2, H_2O, and hydrocarbons on the accurate experimental determination of the rate coefficient of reaction 3 is discussed. Using rate coefficients for reactions 1 and 2 obtained via quantum chemical calculations, we have been unable to model the extent of decomposition of SO_2 measured in a shock tube study of reaction between SO_2 and CO [Bauer, S. H.; Jeffers, P.; Lifshitz, A.; Yadava, B. P. *Proc. Combust. Inst.* **1971**, *13*, 417]. In light of the known sensitivity of reaction 3 to trace impurities, we have incorporated trace amounts of H_2, CH_4, or H_2O, together with our rate coefficients for (1) and (2), in a kinetic model of Alzueta et al. [*Combust. Flame* **2001**, *127*, 2234], which is then shown to be able to substantially model the SO_2 data of Bauer et al. In the course of this modeling study we also computed heats of formation for a number of sulfur-containing small molecules: HS, HSO, HSOH, HOSO, HS_2, HSO_2, $HOSO_2$, HOSOH, and HOSHO.

Introduction

There is recent renewed interest in the high temperature chemistry of sulfur in combustion systems, especially involving coals and petroleum products. Under combustion conditions, sulfur is largely found as sulfur dioxide and this compound can react with carbon monoxide especially under moist conditions. The interaction between SO_2 and CO has been studied extensively experimentally in flow reactors and flames, and kinetic models for the C/H/O/N/S system have been developed.[1−5] Sulfur dioxide is known to inhibit CO oxidation through removal of O atoms and also by catalyzing recombination of H atoms.[1,3,5] Alzueta et al.[5] have additionally found that under near stoichiometric conditions, SO_2 can promote the oxidation of CO. In the development of kinetic models to simulate the oxidation of moist CO containing SO_2, significant sensitivity is generally reported for the reaction

$$SO_2 + CO \rightarrow SO(^3\Sigma^-) + CO_2 \qquad (1)$$

tacitly assumed to be an elementary bimolecular process. The rate coefficient for reaction 1 has been taken by most authors from an early shock tube measurement of Bauer et al.[6] between 1770 and 2450 K and used as $k_1 = 2.7 \times 10^{12} \exp(-48.3 \text{ kcal mol}^{-1}/RT)$ cm^3 mol^{-1} s^{-1}. Bauer et al. studied the reaction between CO and SO_2 diluted in argon in a single pulse shock tube. Only small conversions of CO were studied, hence precluding precise determination of the stoichiometry of the reaction between SO_2 and CO to be made; however, they found that close to 2 mol of CO_2, the major product, were produced for every mole of SO_2 that disappeared. The conditions of the shock tube experiments did not allow quantification of S, although traces of solid sulfur were found on the shock tube walls. Bauer et al. obtained an empirical rate coefficient for reaction between SO_2 and CO; its value is that subsequently quoted in the literature for reaction 1, although they did not claim the mechanism was that of (1). Rather, they favored a multistep process involving vibrational excitation of SO_2 and/or CO.

There do not appear to be any more recent investigations of the mechanism of reaction between SO_2 and CO. In the present work we report on our ab initio quantum chemical and transition-state kinetic analysis of the reaction between SO_2 and CO. Because SO, the assumed product of reaction 1, is also able to oxidize CO, we have additionally analyzed the reaction

$$CO + SO(^3\Sigma^-) \rightarrow CO_2 + S(^3P) \qquad (2)$$

which is analogous with the oxidation reaction

$$CO + O_2 \rightarrow CO_2 + O(^3P) \qquad (3)$$

and a quantum chemical analysis of this reaction is also given.

* Corresponding author. E-mail: j.mackie@chem.usyd.edu.au.

10.1021/jp045086n CCC: $30.25
Published on Web 02/15/2005

Theory and Computational Methods

Quantum Chemical Calculations of Thermochemistry. The geometries, energies and harmonic vibrational frequencies (and hence heats of formation) of all reactants, products, intermediates and transition states were determined at the Gaussian-3//B3LYP (G3//B3LYP) level of theory,[7] whereby equilibrium geometries and vibrational frequencies (scaled by 0.96 in the calculation of zero point and thermal corrections) are obtained by B3LYP/6-31G(d) density functional calculations. The validity of a given transition state structure was confirmed, where necessary, by intrinsic reaction coordinate analyses. The electronic energies were calculated by the G3 approach,[8] i.e., approximating QCISD(T,Full)/G3large energies by a QCISD(T)/6-31G(d) calculation plus basis set corrections evaluated at MP4 and MP2 levels. A higher level correction (based on the number of valence electrons with a and b spins) and spin−orbit corrections applied to open shell atoms complete the G3 protocol.

For a number of species, including transition states, the electronic energies were also computed by the application of Coupled Cluster Theory with single and double excitations and perturbative corrections for triples [CCSD(T)].[9,10] In the case of open shell systems the spin-restricted RCCSD(T) approach was used where the reference states were generated by the Restricted Open Shell Hartree−Fock (ROHF) method,[10] in conjunction with the correlation consistent basis sets of Dunning et al.[11−13] The (R)CCSD(T)/cc-pVTZ and (R)CCSD(T)/cc-pVQZ valence correlated energies ($x = 3,4$) are extrapolated to the complete basis (CBS, $x = \infty$) limit according to[14]

$$E(x) = A + Bx^{-3} \tag{4}$$

Core and core-valence correlation corrections were obtained via (R)CCSD(T)/cc-pCVTZ calculations. Scalar relativistic corrections were evaluated via the Douglas-Kroll formalism[15,16] at the (R)CCSD(T)/cc-pVTZ level of theory.

The G3//B3LYP and (R)CCSD(T) calculations were carried out using the Gaussian03[17] and MOLPRO[18] packages respectively on DEC alpha 600/5/333 and COMPAQ XP100/500 workstations of the Theoretical Chemistry group at the University of Sydney and on the COMPAQ AlphaServer SC system of the Australian Partnership for Advanced Computing National Facility at the National Supercomputing Centre, ANU, Canberra.

Derivation of Rate Coefficients of Individual Reaction Channels. As discussed below, there are two transition states (TS) for both reactions 1 and 2. For the first reaction there is a concerted process taking place via a cis- configuration of an OSOCO TS initially on a singlet surface. Reaction 1 can also take place on a *trans*- surface via a very weakly bound OSOCO intermediate. Rate coefficients have been evaluated using Transition State Theory,[19] ignoring in the second case, the very shallow well of the *trans*-OSOCO intermediate. Similarly, reaction 2 can take place by concerted reaction via a *cis*-SOCO TS or via a weakly bound *trans*-SOCO intermediate. Again, this shallow well has been ignored in the derivation of rate coefficients for reaction 2.

Results and Discussion

Potential Energy Surfaces and Reaction Paths. The results of the G3//B3LYP calculations, viz. total energies (including zero point correction), E_0, atomization energies, ΣD_0, enthalpies of formation at 0 and 298K, rotational constants and (scaled) vibrational frequencies of the reactants, products, intermediates and transition states which constitute reactions 1 and 2 are summarized in Table 1, along with several other sulfur containing species which occur in the overall kinetic model. The structures and geometric parameters of the key transition state and intermediate species are provided in Figure 1 and Table 2.

Comparison of the calculated G3//B3LYP heats of formation in Table 1 with experimental and other computed values indicates that for a number of sulfur-containing species, e.g., SO_2, HOSO, $HOSO_2$, and HOSOH, the current calculated values are higher by $\sim$2−3 kcal mol^{-1}. A simple remedy proposed by Curtiss et al.[27] is an additional basis set correction applied at the SCF level, which consists of the addition of a single 5*g* Gaussian ($\zeta = 0.683$) to the sulfur G3Large basis. This is in fact a key step in the G3X procedure. As the results in Table 1 demonstrate, the "*g*(S) correction" improves the accuracy of the predicted heats of formation by up to 1.7 kcal mol^{-1}, although, due to cancellations between reactants, intermediates and products, the net effect on barrier heights and reaction enthalpies is considerably smaller.

In all subsequent calculations of rate coefficients and kinetic modeling studies, the G3//B3LYP heats of formations are used, so as to maintain internal consistency, not because we regard them as superior to the available experimental values. However, for species such as HOSOH and HOSHO, in the absence of accurate experimental or high level theoretical data, the current G3//B3LYP values with *g*(S) correction are proposed as reliable heats of formation, with estimated errors of ±2 kcal mol^{-1}.

The results of the G3//B3LYP calculations with respect to key barrier heights, reaction energies and the stability of a cyclic form of SO_2CO are compared with the predictions of the (R)CCSD(T)/CBS approach in Table 3. Extrapolation of the valence correlated (R)CCSD(T) energies to the CBS limit typically results in barriers which are 0.1 to 2.2 kcal mol^{-1} higher than obtained with the cc-pVQZ basis. Similar effects are noted for the reaction energies of CO + SO_2 and CO + SO. Core-valence correlation has a substantial ($\sim$0.5 kcal mol^{-1}) effect on the reaction energies, but less on barrier heights, whereas scalar relativistic corrections are just 0.1−0.14 kcal mol^{-1}. In most cases the total CBS energies, including zero point corrections, agree with the G3//B3LYP values to within $\sim$1 kcal mol^{-1}, providing a convincing validation of the applicability of the G3 type approach (with or without the *g*(S) correction) to the current systems of interest. The obvious exception is the barrier height corresponding to the *trans*-SO_2CO TS2 ($^3A''$) species, where the RCCSD/CBS estimate is 2.7 kcal mol^{-1} higher than the G3//B3LYP value. Given the complex nature of the results which are derived via composite calculations, we cannot offer an explanation for this discrepancy. On the other hand, we find that the scalar relativistic corrections to reaction energies and barrier heights, which are not included in G3, are negligible. For consistency in the kinetic modeling, we employ the G3 results.

In the study of reaction 1 two stable adducts between CO and SO_2 were located: a closed shell cyclic form and an open chain OC−OSO biradical species, which are readily described by the Lewis structures:

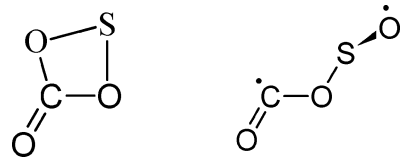

The ground state of the *trans*- open chain adduct is found to be singlet, which is calculated to be 0.6 kcal mol^{-1} more stable then the analogous triplet biradical. Because the G3 and re-

TABLE 1: G3//B3LYP Total Energies, Atomization Energies, Heats of Formation, Rotational Constants, and Harmonic Vibrational Frequencies of Reactants, Products, Intermediates, and Transition States

	rotational constants/cm^{-1}	frequencies/cm^{-1}	E_0/E_h	$\sum D_o$/ kcal mol^{-1}	$\Delta_f H^0_0$/ kcal mol^{-1}	$\Delta_f H^0_{298}$/kcal mol^{-1}		
						g(S) uncorr	g(S) corr	lit.
SO_2 ($^1A_1$)	1.918, 0.331, 0.282	482, 1095, 1284	−548.42774	251.5	−67.8	−68.1	−69.0	−70.9[a]
SO ($^3\Sigma^-$)	0.687	1078	−473.19100	123.2	1.5	1.7		1.2[a]
CO_2 ($^1\Sigma_g^+$)	0.386	615, 615, 1317, 2339	−188.50435	383.6	−95.6	−95.4		−94.1[a]
CO ($^1\Sigma^+$)	1.899	2121	−113.26997	256.8	−27.8	−26.8		−26.4[a]
cis-SO_2CO TS (^1A)	0.309, 0.107, 0.084	821*i*, 87, 119, 298, 373, 548, 696, 1101, 1892	−661.60512	450.2	−37.6	−37.5	−39.0	
trans-SO_2CO TS1 (^1A)	0.588, 0.070, 0.064	734*i*, 73, 179, 248, 357, 440, 753, 1098, 1907	−661.60615	450.8	−38.2	−38.1	−39.3	
trans-SO_2CO Eq^m(^1A)[b]	0.547, 0.075, 0.068	76, 172, 191, 354, 466, 703, 886, 1095, 1817	−661.60715	451.4	−38.8	−38.6		
trans-SO_2CO Eq^m(^3A)	0.590, 0.073, 0.068	57, 175, 236, 336, 475, 734, 978, 1097, 1825	−661.60620	450.8	−38.2	−38.0	−39.5	
trans-SO_2CO TS2 ($^3A''$)	0.433, 0.081, 0.068	729*i*, 117, 145, 265, 384, 693, 871, 1124, 1828	−661.59322	442.7	−30.1	−30.1	−31.5	
cycl SO_2CO Eq^m($^1A_1$)	0.463, 0.124, 0.098	222, 469, 597, 664, 700,767, 933, 1076, 1893	−661.65193	479.5	−66.9	−67.6	−68.9	
cycl SO_2CO TS ($^1A'$)	0.372, 0.114, 0.087	679*i*, 124, 287, 379, 516,598, 911, 1143, 2113	−661.61091	453.8	−41.2	−41.5	−42.9	
cis-SOCO TS ($^3A''$)	0.695, 0.134, 0.112	795*i*, 48, 218, 548, 748, 1904	−586.38563	332.7	20.9	21.4	20.8	
trans-SOCO TS1 ($^3A''$)	2.629, 0.095, 0.092	646*i*, 107, 264, 426, 835, 1899	−586.38860	334.6	19.1	19.4	18.7	
trans-SOCO Eq^m($^3A''$)	2.596, 0.100, 0.097	148, 238, 482, 791, 871, 1829	−586.39155	336.4	17.2	17.6	16.9	
trans-SOCO TS2 (^3A)	0.994, 0.118, 0.109	189*i*, 218, 516, 559, 745, 1846	−586.38477	332.2	21.5	21.5	20.7	
HS ($^2\Pi$)	9.395	2569	−398.59664	83.5	33.7	33.6,	33.5	33.3[a]
HSO ($^2A''$)	9.918, 0.649, 0.609	939, 1033, 2337	−473.78273	180.1	−3.8	−4.5	−5.0	−4.4 ±1.5[c]
HSOH (^1A)	6.622, 0.494, 0.481	486, 723, 961, 1192, 2504, 3569	−474.39953	252.7	−24.8	−26.6	−27.2	−28.5[d]
HOSO (^2A)	1.145, 0.298, 0.239	144, 363, 720, 1049, 1101, 3524	−548.99108	290.5	−55.3	−56.3	−57.4	−57.7[e]
HS_2 ($^2A''$)	9.851, 0.255, 0.248	548, 884, 2464	−796.67321	155.2	27.8	27.1	26.6	25.8 ± 2.5[f]
HSO_2 (^2A)	1.628, 0.301, 0.263	423, 769, 937 987, 1173, 2212	−548.95396	267.2	−32.0	−33.4	−34.5	−33.8[e]
$HOSO_2$ (^2A)	0.297, 0.287, 0.156	239, 375, 384, 482, 696, 1011, 1081, 1201, 3534	−624.16119	377.0	−82.8	−84.4	−86.1	−89.1 ± 1.4[g]
HOSOH (^1A)	0.856, 0.272, 0.215	307, 507, 523, 739, 748, 1172, 1176, 3536, 3538	−549.58746	350.3	−63.4	−65.8	−66.9	−69.3[h]
HOSHO (^1A)	1.065, 0.274, 0.232	322, 398, 686, 948, 1073, 1131, 1202, 2318, 3558	−549.57887	344.9	−58.0	−60.5	−61.6	
H_2S_2 (^1A)	4.849, 0.224, 0.224	417, 475, 868, 869, 2528, 2529	−797.28927	227.3	7.3	5.5	4.8	
S (^3P)			−397.96241		65.7[a]			66.2[a]
O (^3P)			−75.03229		59.0[b]			59.6[a]
C (^3P)			−37.82845		170.0[a]			171.3[a]
H (^2S)			−0.50109		51.6[a]			52.1[a]

[a] Experiment, ref 20. [b] Electronic energy based on G3//B3LYP energy of *trans*-SO_2CO Eq^m(^3A) plus MRCI/cc-pVTZ estimate of singlet−triplet separation (see text). [c] CBS calc, ref 21. [d] G2 calc, ref 22. [e] G2 calc, ref 23. [f] CCSD(T)/CBS calc, ref 24. [g] Experiment, ref 25. [h] G3(MP2) calc, ref 26.

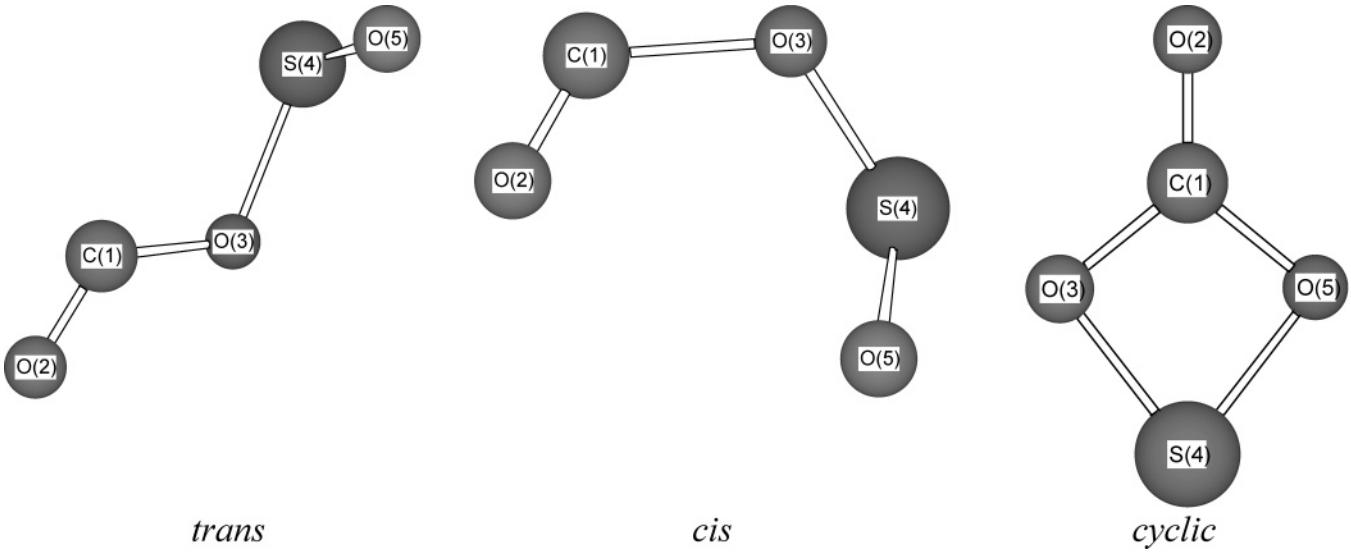

Figure 1. Structures of *trans*-SO_2CO, *cis*-SO_2CO and cyclic SO_2CO. The trans and cis isomers of SOCO are derivable from these structures by deleting O(5).

lated methods are not directly applicable to singlet biradicals, the energy of the latter was obtained by computing (using MOLPRO[18]) the singlet−triplet separation via multireference configuration interaction (MRCI) theory[28,29] (including Davidson's correction[30,31]), with the cc-pVTZ basis. The computed MRCI splitting was then added to the G3//B3LYP energy of the triplet state. The geometry and frequencies of this singlet biradical were obtained at the UB3LYP/6-31G(d) level of theory. As the data in Tables 1 and 2 show, the singlet and triplet states have nearly the same geometries, vibrational frequencies and stabilities. More importantly, the singlet equilibrium structure is very weakly bound. It lies just 0.6 kcal mol^{-1} lower than the reverse barrier to dissociation (to CO + SO_2). No equivalent cis equilibrium structure was located, only a singlet transition state which suggests that on the cis surface reaction 1 is a concerted process, whereas on the trans surface there are two transition states which are associated with the formation of the OC−OSO adduct and its dissociation to CO_2 + SO, respectively. A similar scenario appears to apply to reaction 2, inasmuch as there are two reaction pathways, cis-

TABLE 2: Geometries of Transition States and Equilibrium Geometries of SO_2CO and SOCO Adducts Computed at B3LYP/6-31G(d) Level of Theory[a]

	cis-SO_2CO TS (^1A)	*trans*-SO_2CO TS1 (^1A)	*trans*-SO_2CO Eq^m(^1A)	*trans*-SO_2CO Eq^m(^3A)	*trans*-SO_2CO TS2 ($^3A''$)	cycl SO_2CO Eq^m($^1A_1$)	cycl SO_2CO TS ($^1A'$)	*cis*-SOCO TS ($^3A''$)	*trans*-SOCO TS1 ($^3A''$)	*trans*-SOCO Eq^m($^3A''$)	*trans*-SOCO TS2 (^3A)
*R*C1−O2	1.164	1.163	1.182	1.183	1.196	1.186	1.160	1.162	1.165	1.180	1.174
*R*C1−O3	1.586	1.558	1.375	1.366	1.286	1.373	1.240	1.586	1.550	1.391	1.430
*R*S4−O3	1.632	1.624	1.722	1.738	1.944	1.738	2.018	1.636	1.627	1.680	1.675
*R*S4−O5	1.489	1.490	1.492	1.491	1.488	1.738	1.576				
θO2−C1−O3	123.8	120.2	125.4	125.9	134.2	129.0	153.3	126.1	119.3	124.1	126.7
θC1−O3−S4	117.6	126.2	120.2	114.7	110.4	91.1	93.7	118.1	122.4	117.6	116.5
θO3−S4−O5	112.2	111.6	109.4	108.9	105.1	75.8	83.5				
τO2−C1−O3−S4	34.9	−170.8	−174.6	−179.7	180.0	180.0	180.0	0.0	180.0	180.0	88.7
τC1−O3−S4−O5	−64.9	73.5	61.7	85.2	0.0	0.0	0.0				

[a] Distances given in Å, angles in degrees. See Figure 1 for schematic structures and labeling of atoms.

TABLE 3: Comparison of G3//B3LYP and CCSD(T)/CBS Barrier Heights and Reaction Energies (in kcal mol^{-1}) and Core-Valence Correlation (CV), Scalar Relativistic, and Zero Point Energy (ZPE) Contributions to the CCSD(T)/CBS Energies[a]

	ΔE			$\Delta\Delta E$			ΔE_0		
	(R)CCSD(T)/cc-pVTZ	(R)CCSD(T)/cc-pVQZ	(R)CCSD(T)/CBS	CV	relativity	ZPE	CBS	G3//B3LYP	G3//B3+g(S)
cis-SO_2CO TS − (SO_2 + CO)	55.71	57.37	58.59	0.20	−0.11	0.19	58.86	58.10	57.49
trans-SO_2CO TS1 − (SO_2 + CO)	54.77	56.44	57.66	0.20	−0.07	0.10	57.89	57.50	57.17
trans-SO_2CO TS2 − (SO_2 + CO)	62.86	65.88	68.09	−0.29	−0.14	0.64	68.30	65.60	65.15
cycl-SO_2CO Eq^m − (SO_2 + CO)	17.92	21.84	24.70	−0.45	−0.02	3.35	27.57	28.70	28.29
(SO + CO_2) − (SO_2 + CO)	−6.12	−1.36	2.12	−0.45	−0.10	1.40	2.97	1.50	1.98
cis-SOCO TS − (SO + CO)	47.29	47.41	47.50	0.01	0.02	0.38	47.92	47.28	47.10
trans-SOCO TS1 − (SO + CO)	44.90	45.02	45.10	−0.05	0.05	0.48	45.58	45.42	45.11
trans-SOCO TS2 − (SO + CO)	46.36	46.48	46.57	−0.14	0.08	0.98	47.49	47.82	47.38
(S + CO_2) − (SO + CO)	−9.86	−7.60	−5.95	−0.38	0.01	2.41	−3.91	−3.63	−4.07

[a] ΔE_0(CBS) = ΔE(CCSD(T)/CBS) + $\Delta\Delta E$(CV) + $\Delta\Delta E$(Rel) + $\Delta\Delta E$(ZPE).

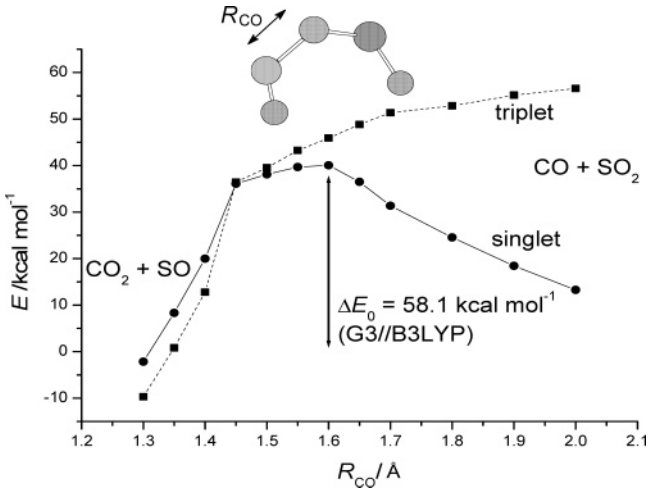

Figure 2. B3LYP/6-31G(d) singlet and triplet potential energy surfaces for reaction 1 via *cis*-SO_2CO TS.

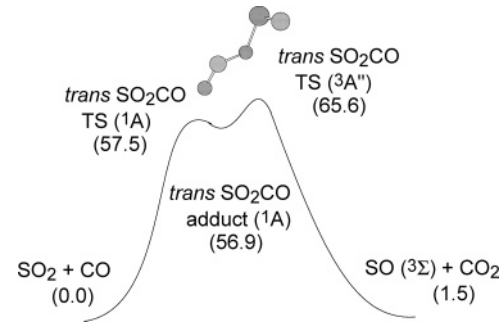

Figure 3. Schematic potential energy surface for reaction 1 via trans adduct and transition states with G3//B3LYP relative energies (kcal mol^{-1}).

and trans-, describing the oxygen abstraction by CO, with a slightly stable OC-OS adduct located only on the trans- surface.

As the reactants in reaction 1 are both singlets, and the products in the state of lowest energy are $CO_2(^1\Sigma)$ + $SO(^3\Sigma)$, the reaction involves singlet−triplet surface crossing. In an effort to determine whether the intersystem crossing may be rate determining, we have investigated the cis- potential energy surface as a function of the forming C−O bond length as the reaction passes through the *cis*-SO_2CO TS. Figure 2 shows the variation in B3LYP/6-31G(d) singlet and triplet energies versus the critical CO distance. The reaction starts out on the singlet surface, with a large CO distance (on the right of the figure) and initially follows this surface as the forming CO bond shortens and passes through the barrier whose height is 58.1 kcal mol^{-1} (computed at the higher level G3//B3LYP) on the singlet surface. At the barrier the molecular wave function effectively corresponds to a closed shell configuration which can be described by single reference treatments, such as CCSD(T), QCISD(T) and Møller−Plesset Perturbation Theory. The intersystem crossing is predicted to occur at a significantly lower energy at a CO bond length which is 0.15 Å shorter than in the singlet transition state. The reaction then exits on the lower-lying triplet surface. The rate coefficient, obtained via transition state theory, is therefore assumed to be determined by the rate of crossing the singlet barrier.

As noted above, reaction 1 can also proceed on a *trans*-surface leading to a metastable singlet OCOSO intermediate (via a singlet transition state *trans*-SO_2CO TS1), although the stabilization of this adduct appears to be only 0.6 kcal mol^{-1}. There is, however, a further significant barrier ($\sim$ 8 kcal mol^{-1}), involving the *trans*-$SO_2CO(^3A'')$ TS2 species, to dissociation to $SO(^3\Sigma)$ and ground-state CO_2. The qualitative features of this surface are depicted in Figure 3. As in the case of the cis-isomer, the first transition state TS1 is effectively a closed-shell system, which then rapidly evolves into the open-shell

biradical species, viz. the equilibrium structure. The intersystem crossing is expected to occur at an intermediate geometry (between the equilibrium and the second transition state geometries) and hence it is not expected to be rate determining. Given the large difference between the highest barriers on the cis and trans surfaces ($\sim$ 7.5 kcal mol^{-1} at the G3//B3LYP level and even higher at the (R)CCSD(T)/CBS level), the rate of reaction 1 can be expected to be determined almost entirely by the cis pathway.

As the results in Table 1 show, cyclic SO_2CO ($^1A_1$) is $\sim$ 29 kcal mol^{-1} more stable than the open chain molecules. As the former may be expected to arise by a simple ring closure reaction of *trans*-SO_2CO, we investigated the energetics of such a process by performing relaxed scans of the potential energy surface as a function of the O3−S4−O5 angle, decreasing it from 109° toward $\sim$ 76° which it would adopt in the cyclic structure. We found that such a process results in a gradual increase in the O3−S4 distance and an increase in the total energy, so that at $\sim$ 90°, where the energy exceeds that of the barrier TS2, dissociation to CO_2 + SO results. Consideration of the reverse, viz. ring opening reaction of cyclic SO_2CO, by systematic stretch of the C1−O5 bond did yield a transition state (denoted cycl SO_2CO TS in Tables 1 and 2), but rather than corresponding to a ring-opening reaction, it leads to dissociation to CO_2 + SO. This was verified by an intrinsic reaction coordinate analysis, although it is quite obvious from a consideration of the normal mode corresponding to the imaginary frequency and even from the geometry. The C1−O5 and O3−S4 distances in the transition state are 1.95 and 2.02 Å, respectively. The formation of cyclic SO_2CO thus constitutes a further, subsequent reaction of the product molecules SO and CO_2 which, however, would not affect the rate of disappearance of SO_2 or CO. In other words, the reaction is not relevant to the problem addressed in this work.

Reaction (2), between SO and CO, takes place on triplet surfaces. There is a concerted reaction passing through a *cis*-SOCO TS, whereas the reaction on the trans surface leads to a weakly stable complex, with a well depth $\sim$2 kcal mol^{-1}. On the trans surface thus there is a further small barrier ($\sim$4 kcal mol^{-1}) involving a trans−cis isomerization with eventual dissociation on the cis surface to CO_2 + S(^{3}P). Qualitatively, these reactions resemble those of SO_2 + CO, but without the singlet−triplet intersystem crossing. The SOCO structures discussed above have been previously identified by Froese and Goddard,[32] in their study of the OCS + O reaction, using MP2 and MP4 methods. They also identified the global minimum as a singlet cyclic isomer S═(COO), where the (COO) moiety has a ring structure.

Kinetic Parameters. Rate coefficients have been evaluated individually using transition state theory for reactions taking place on both the cis and trans surfaces pertaining to reactions 1 and 2 using the G3//B3LYP heats of formation and other relevant data. In the case of the two reactions on trans surfaces, the very shallow wells have been ignored and the final barriers shown in Figures 2 and 3 have been adopted. Rate coefficients have been computed for the temperature range of 1000−3000 K and are well fitted over this region by the Arrhenius parameters given in Table 4.

Comparison with Experiment. Our rate coefficients for reaction 1 are approximately an order of magnitude lower at 2000 K than the value derived by Bauer et al.[6] and we have been unable to model their SO_2 yields in their single pulse shock tube studies using just the two rate coefficients for the two reactions, (1) and (2). Our activation energies for reaction 1 are considerably higher than reported in the experiments,[6] yet we consider that our G3//B3LYP calculations should yield barriers accurate to 1−2 kcal mol^{-1}. Before attempting to address this discrepancy between theory and experiment for oxidation of CO by SO_2, we reconsider the oxidation of CO by O_2, (3), a reaction that exhibits analogies especially with reaction 2.

TABLE 4: Arrhenius Parameters Derived from the G3//B3LYP Quantum Chemical Calculations

reaction no.	reactions	A/cm^3 mol^{-1} s^{-1}	E_a/kcal mol^{-1}
1 (cis)[a]	$SO_2 + CO \rightarrow SO + CO_2$	1.94×10^{13}	65.9
1(trans)[a]	$SO_2 + CO \rightarrow SO + CO_2$	2.67×10^{13}	72.7
2 (cis)[a]	$CO + SO \rightarrow CO_2 + S(^3P)$	5.10×10^{13}	53.4
2 (trans)[a]	$CO + SO \rightarrow CO_2 + S(^3P)$	3.91×10^{12}	53.3

[a] Configuration of transition state.

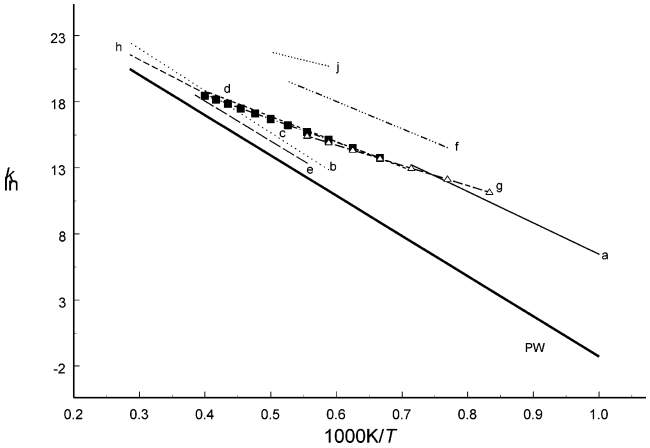

Figure 4. Comparison between experimental rate coefficients for reaction 3, a−j, and our ab initio derived rate coefficient, PW: (a) ref 38; (b) ref 35; (c) ref 39; (d) ref 40; (e) ref 36; (f) ref 41; (g) ref 42; (h) ref 43; (j) ref 44.

Measurements of the rate coefficient for reaction 3 are several and varied, as can be ascertained from the NIST tabulation.[33] We have also carried out quantum chemical calculations on reaction 3 at the G3//B3LYP level of theory and arrive at the rate coefficient of $k_3 = 4.7 \times 10^{12} \exp(-60.5 \text{ kcal mol}^{-1}/RT)$ cm^3 mol^{-1} s^{-1} between 1000 and 3000 K. Our value is compared with previous experimental values in Figure 4. There is a great degree of variation among the experimental data, and the theoretical value is significantly lower than experiment. It should be noted, however, that nearly all of the values for k_3 shown in Figure 4 were obtained from shock tube studies on $H_2/CO/O_2/Ar$ mixtures and detailed chemical kinetic modeling was required to isolate the kinetics of reaction 3 from the very rapid oxidation of CO by OH

$$CO + OH \rightarrow CO_2 + H \quad (5)$$

and the (less important) recombination of O and CO:

$$CO + O + M \rightarrow CO_2 + M \quad (6)$$

Several of the data, especially those exhibiting large values of k_3 at relatively low temperatures, undoubtedly show the influence of reaction 5 and possibly (6). Indeed, Clark, Dean, and Kistiakowski[34] showed several years ago that very small traces of organic impurities can catalyze reaction 3 significantly. It is only in the study by Thielen and Roth[35] that reaction 3 has been studied under relatively clean conditions. However, even in those studies, small concentrations of H and O were detected and these

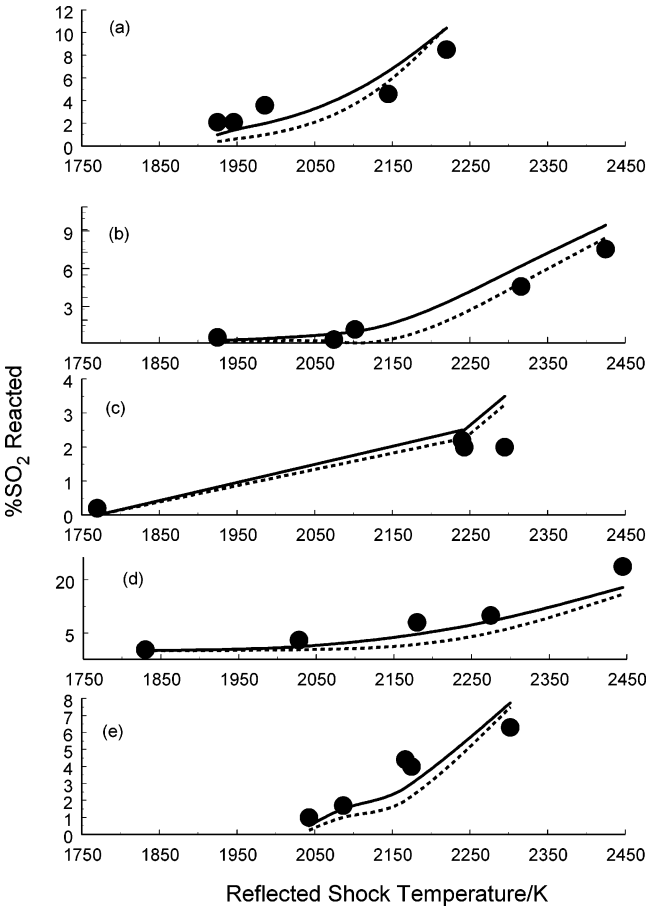

Figure 5. Comparison between experimental $\%SO_2$ reacted versus reflected shock temperature and modeled data with an impurity of 0.02 mol % of H_2 (dashed lines) and of 0.008 mol % of CH_4 (solid lines): (a) 1.0% CO + 1.0%SO_2 in Ar, pressures 9.0−9.6 atm; (b) 1.0% CO + 1.0%SO_2 in Ar, pressures 1.8−3.3 atm; (c) 1.0% CO + 4.0%SO_2 in Ar, pressures 3.0−3.7 atm; (d) 4.0% CO + 1.0%SO_2 in Ar, pressures 2.7−3.2 atm; (e) 4.0% CO + 4.0%SO_2 in Ar, pressures 1.7−3.4 atm. Data from ref 6.

atoms could contribute to catalysis of reaction 3. Our ab initio results for k_3 yield similar activation energies to those found by Dean and Kistiakowski[36] and Thielen and Roth[35] although our rate coefficients are lower than those of the earlier workers by a factor of about 3 and 5, respectively, at 2000 K. It is possible that both of these experimental studies are still slightly affected by catalysis by trace impurities and that a measurement of the rate coefficient of reaction 3 totally unaffected by trace impurities might be highly difficult to perform.

With this background we turn to a discussion of the rate coefficients we have computed for reactions 1 and 2. Bauer et al.[6] conducted their CO/SO_2 experiments with CP carbon monoxide. However, Dean and Kistiakowski[36] specifically caution that there are "kinetically significant concentrations of impurities" in CP carbon monoxide. One possibility is that the significantly larger rate coefficients found by Bauer et al.[6] might be a consequence of traces of impurities in their reagent gases. To gauge the effects of small concentrations of impurities, we have carried out kinetic modeling on the CO/SO_2 system with small added concentrations of H_2, H_2O, or CH_4, all possible trace impurities in a sample of CP carbon monoxide.

The S/O/C/H mechanism we have employed is similar to that presented by Alzueta, Bilbao, and Glarborg[5] with thermochemistry of sulfur-containing species calculated in the present work. To this mechanism we have added the four rate coefficients from Table 4. Modeling was performed by the SENKIN code.[37]

Figure 5 shows the effects of addition of 0.02 mol % of H_2 and separately, the effects of addition of 0.008 mol % of CH_4 on the modeling of the oxidation of CO/SO_2 mixtures studied under the experimental conditions of Bauer et al.[6] Without the addition of either of these "impurities", use of the rate coefficients of Table 4 would lead to a gross underprediction of the extent of decomposition of SO_2 (by a factor of about 10 at the lowest temperatures and of about 3 at the highest temperatures of Figure 5). However, the presence of either H_2 or CH_4 at the above levels leads to predictions of the $\%SO_2$ reacted that are close to those measured by Bauer et al.[6] Water added at a level of approximately 3 times that of H_2 also leads to a comparable extent of decomposition of SO_2.

Sensitivity analysis enables a quantitative understanding of how variation in an individual rate coefficient in a reaction model can affect the computed species concentration(s). Most sensitive reactions have the largest normalized sensitivity coefficients, $S_{ij} = \partial \ln c_j / \partial \ln k_i$, where k_i is the rate coefficient of the ith reaction and c_j is the concentration of the jth species.[37] Sensitivity analysis as performed by SENKIN on the reaction model reveals that for CH_4, added at the level of 0.008 mol %, the most sensitive reaction for disappearance of SO_2 and/or CO is the reaction

$$SO + OH \rightarrow SO_2 + H \qquad (7)$$

and the reaction

$$OH + CO \rightarrow H + CO_2 \qquad (5)$$

also exhibits moderate sensitivity. At early stages of the reaction, at 20 μs after passage of the shock front, there is some sensitivity to the two rate coefficients for reaction 1. However, at later stages of the reaction (>100 μs), this sensitivity to k_1 disappears. In the cases of H_2 (0.02 mol %) and H_2O (0.06 mol %), both rate coefficients for reaction 1 are quite sensitive at early stages of reaction. However, as reaction progresses, this sensitivity is lost and reactions 7 and 5 become most sensitive in the case of added H_2. With added H_2O, however, it is the chain-branching reaction

$$O + H_2O \rightarrow 2OH \qquad (8)$$

that becomes most sensitive. The oxidation reactions of SO, namely

$$SO + O_2 \rightarrow SO_2 + O \qquad (9)$$

and reaction 7 also become sensitive reactions as reaction progresses.

Our modeling demonstrates the extreme sensitivity of the CO/SO_2 reaction to small amounts of impurities such as H_2, H_2O, and traces of organic materials like methane, which can lead to chain branching producing radicals such as OH, H, and O that can accelerate the oxidation of CO and the decomposition of SO_2. Because most of the practical combustion systems containing CO and SO_2 are moist and often contain hydrocarbon fuels, the rate of oxidation of CO in these systems would be expected to be much faster than the intrinsic rate of reaction 1.

Conclusion

Our quantum chemical studies suggest that the barrier to oxidation of CO by SO_2 (and by O_2) is significantly higher than that reported by experiment. Because the oxidation of CO is significantly accelerated by the presence of impurities such as

H_2, H_2O, or traces of hydrocarbons, reaction 1 is likely to be irrelevant in the oxidation of *moist* carbon monoxide.

References and Notes

(1) Kallend, A. S. *Combust. Flame* **1969**, *13*, 227.

(2) Smith, O. I.; Wang, S.-N.; Tseregounis, S.; Westbrook, C. K. *Combust. Sci. Technol.* **1983**, *30*, 241.

(3) Glarborg, P.; Kubel, D.; Dam-Johansen, K.; Chiang, H. M.; Bozzelli, J. W. *Int. J. Chem. Kinet.* **1996**, *28*, 773.

(4) Mueller, M. A.; Yetter, R. A.; Dryer, F. L. *Int. J. Chem. Kinet.* **2000**, *32*, 317.

(5) Alzueta, M. U.; Bilbao, R.; Glarborg, P. *Combust. Flame* **2001**, *127*, 2234.

(6) Bauer, S. H.; Jeffers, P.; Lifshitz, A.; Yadava, B. P. *Proc. Combust. Inst.* **1971**, *13*, 417.

(7) Baboul, A. G.; Curtiss, L.; A.Redfern, P. C.; Raghavachari, K. *J. Chem. Phys.* **1999**, *110*, 7650.

(8) Curtiss, L. A.; Raghavachari, K.; Redfern, P. C.; Rassolov, V.; Pople, J. A. *J. Chem. Phys*. **1998**, *109*, 7764.

(9) Raghavachari, K.; Trucks, G. W.; Pople, J. A.; Head-Gordon, M. *Chem. Phys. Lett.* **1989**, *157*, 479.

(10) Hampel, C.; Peterson, K. A.; Werner, H.-J. *Chem. Phys. Lett.* **1992**, *190*, 1.

(11) Dunning, T. H., Jr. *J. Chem. Phys.* **1989**, *90*, 1007.

(12) Kendall, R. A.; Dunning, T. H., Jr.; Harrison, R. J. *J. Chem. Phys.* **1992**, *96*, 6796.

(13) Woon, D. E.; Dunning, T. H., Jr. *J. Chem. Phys.* **1993**, *98*, 1358.

(14) Helgaker, T.; Klopper, W.; Koch, H.; Noga, J. *J. Chem. Phys.* **1997**, *106*, 9639.

(15) Douglas, M.; Kroll, N. M. *Ann. Phys. (N. Y.)*, 1974, *82*, 89.

(16) Hess, B. A. *Phys. Rev. A.* **1986**, *33*, 3742.

(17) Frisch, M. J.; Trucks, G. W.; Schlegel, H. B.; Scuseria, G. E.; Robb, M. A.; Cheeseman, J. R.; Montgomery, J. A., Jr.; Vreven, T.; Kudin, K. N.; Burant, J. C.; Millam, J.; M.Iyengar, S. S.; Tomasi, J.; Barone, V.; Mennucci, B.; Cossi, M.; Scalmani, G.; Rega, N.; Petersson, G. A.; Nakatsuji, H.; Hada, M.; Ehara, M.; Toyota, K.; Fukuda, R.; Hasegawa, J.; Ishida, M.; Nakajima, T.; Honda, Y.; Kitao, O.; Nakai, H.; Klene, M.; Li, X.; Knox, J. E.; Hratchian, H. P.; Cross, J. B.; Adamo, C.; Jaramillo, J.; Gomperts, R.; Stratmann, R. E.; Yazyev, O.; Austin, A. J.; Cammi, R.; Pomelli, C.; Ochterski, J. W.; Ayala, P. Y.; Morokuma, K.; Voth, G. A.; Salvador, P.; Dannenberg, J. J.; Zakrzewski, V. G.; Dapprich, S.; Daniels, A. D.; Strain, M. C.; Farkas, O.; Malick, D. K.; Rabuck, A. D.; Raghavachari, K.; Foresman, J. B.; Ortiz, J. V.; Cui, Q.; Baboul, A. G.; Clifford, S.; Cioslowski, J.; Stefanov, B. B.; Liu, G.; Liashenko, A.; Piskorz, P.; Komaromi, I.; Martin, R. L.; Fox, D. J.; Keith, T.; Al-Laham, M. A.; Peng, C. Y.; Nanayakkara, A.; Challacombe, M.; Gill, P. M. W.; Johnson, B.; Chen, W.; Wong, M. W.; Gonzalez, C.; Pople, J. A. *Gaussian 03*, Revision B.05; Gaussian, Inc.: Pittsburgh, PA, 2003.

(18) Amos, R. D.; Bernhardsson, A.; Berning, A.; Celani, P.; Cooper, D. L.; Deegan, M. J. O.; Dobbyn, A. J.; Eckert, F.; Hampel, C.; Hetzer, G.; Knowles, P. J.; Korona, T.; Lindh, R.; Lloyd, A. W.; McNicholas, S. J.; Manby, F. R.; Meyer, W.; Mura, M. E.; Nicklass, A.; Palmieri, P.; Pitzer, R.; Rauhut, G.; Schütz, M.; Schumann, U.; Stoll, H.; Stone, A. J.; Tarroni, R.; Thorsteinsson, T.; Werner, H.-J. MOLPRO: a package of ab initio programs designed by H.-J. Werner and P. J. Knowles; version 2002.6.

(19) Steinfeld, J. I.; Francisco, J. S.; Hase, W. L. *Chemical Kinetics and Dynamics*; Prentice Hall: Engelwood Cliffs, NJ, 1989.

(20) Chase, M. W., Jr. NIST-JANAF Thermochemical Tables, 4th ed. *J. Phys. Chem. Ref. Data* **1998**, *Monograph 9*.

(21) Badenes, M. P.; Tucceri, M. E.; Cobos, C. J. *Z. Phys. Chem*. **2000**, *214*, 1193.

(22) Goumri, A.; Rocha, J.-D. R.; Laakso, D.; Smith, C. E.; Marshall, P. *J. Phys. Chem.* **1994**, *101*, 9405.

(23) Goumri, A.; Rocha, J.-D. R.; Laakso, D.; Smith, C. E.; Marshall, P. *J. Phys. Chem. A* **1999**, *103*, 11328.

(24) Decker, B. K.; Adams, N. G.; Babcock, L. M.; Crawford, T. D.; Schaefer, H. F., III. *J. Phys. Chem. A* **2000**, *104*, 4636.

(25) Blitz, M. A.; Hughes, K. J.; Pilling, M. J. *J. Phys. Chem. A* **2003**, *107*, 1971.

(26) Wang, L.; Zhang, J. *J. Mol. Struct. (THEOCHEM)* **2002**, *581*, 129.

(27) Curtiss, L. A.; Redfern, P. C.; Raghavachari, K.; Pople, J. A. *J. Chem. Phys.* **2001**, *124*, 108.

(28) Werner, H.-J.; Knowles, P. J. *J. Chem. Phys*. **1988**, *89*, 5803.

(29) Knowles, P. J.; Werner, H.-J. *Chem. Phys. Lett*. **1988**, *145*, 514.

(30) Langhoff, S. R.; Davidson, E. R. *Int. J. Quantum Chem*. **1974**, *8*, 61.

(31) Richartz, A.; Buenker, R. J.; Peyerimhoff, S. D. *Chem. Phys*. **1990**, *28*, 305.

(32) Froese, R. D. J.; Goddard, J. D. *Mol. Phys*. **1993**, *79*, 685.

(33) Mallard, W. G.; Westley, F.; Herron, J. T.; Hampson, R. F.; Frizzell, D. H. *NIST Chemical Kinetics Database Windows Version 2Q98*; NIST: Gaithersburg, MD 20899; 1998.

(34) Clark, T. C.; Dean, A. M.; Kistiakowsky, G. B. *J. Chem. Phys.* **1971**, *54*, 1726.

(35) Thielen, K.; Roth, P. *Ber. Bunsen-Ges. Phys. Chem.* **1983**, *87*, 920.

(36) Dean, A. M.; Kistiakowsky, G. B. *J. Chem. Phys.* **1971**, *54*, 1718.

(37) Lutz, A.; Kee, R. J.; Miller, J. A. SENKIN: A Fortran Program for Predicting Homogeneous Gas Phas Chemical Kinetics with Sensitivity Analysis. Sandia National Laboratories Report SAND87-8248, February, 1988.

(38) Koike, T. *Bull. Chem. Soc. Jpn.* **1991**, *64*, 1726.

(39) Rawlins, W. T.; Gardiner, W. C., Jr. *J. Phys. Chem.* **1974**, *78*, 497.

(40) Gardiner, W. C., Jr.; McFarland, M.; Morinaga, K.; Takeyama, T.; Walker, B. F. *J. Phys. Chem.* **1971**, *75*, 1504.

(41) Brabbs, T. A.; Belles, F. E. *Proc. Int. Symp. Shock Tubes Waves* **1971**, *67*, 24.

(42) Drummond, L. J. *Aust. J. Chem*. **1968**, *21*, 2631.

(43) Sulzmann, K. G. P.; Myers, B. F.; Bartle, E. R. *J. Chem. Phys.* **1965**, *42*, 3969.

(44) Fenimore, C. P.; Jones, G. W. *J. Phys. Chem.* **1957**, *61*, 651.